Outage Probability Analysis of Uplink RIS and UAV–Assisted THz Mobile Communications

Sara Farrag
German University in Cairo
sarah.farrag@guc.edu.eg

Engy A. Maher
German University in Cairo
engy.maher@guc.edu.eg

Ahmed El-Mahdy
German University in Cairo
ahmed.elmahdy@guc.edu.eg

Falko Dressler
TU Berlin
dressler@ccs-labs.org

***Abstract*—Reconfigurable intelligent surface (RIS) is considered as a promising low–cost technology that can adaptively control the phase of signals to boost the system performance. For a higher probability of line–of–sight (LOS) between communicating nodes and to substitute for loss due to long distance travelled, an unmanned aerial vehicle (UAV) is deployed. In this paper, we investigate the uplink RIS–assisted communication system in the terahertz (THz) band in the existence of a couple of underlaying device–to–device (D2D) pairs. The RIS is attached to the UAV for a higher mobility and channel gains quality. A closed form expression is derived for the outage probability at the base station (BS) for the considered scenario. The optimum UAV's position that minimizes this outage probability is obtained using Golden Search method. Moreover, the optimum phase shifts of the RIS elements that maximize the signal–to–interference–noise–ratio (SINR) at the BS are obtained. Numerical results are obtained to evaluate the performance of the outage probability of the system. The results show that using the optimum algorithm, the outage probability achieves the minimum value compared to other schemes.**

***Index Terms*—Wireless communication, Outage Probability, UAV, THz, RIS and D2D.**

I. Introduction

With the explosive increase of data traffic in various communication scenarios, evolving modern spectrum resources for near future sixth generation (6G) has become urgently needed [1]. In order to satisfy this ever–increasing bandwidth demands for the 6G application such as wireless data centers, holographic tracking systems, on–chip communications, space communication networks and broadband local area network (LAN), researchers and technology makers started investigating the only existing gap in the frequency spectrum [2]. THz frequency band ranges from 0.1 THz to 10 THz and is allocated between the microwave and infrared bands [3]. The THz frequency range promises huge bandwidth that theoretically reaches up to some THz, which in turn results in potential capacity in the order of Terabits/sec. That is, the bandwidth it provides is one order of magnitude over the millimeter wave (mmWave) band. Furthermore, deploying THz frequency band in today's networks has countless advantages [4]. For instance, THz signals offer higher link directionality and permit lower eavesdropping chances when compared to mmWave signals [5]. THz signals are proved as good candidates for uplink communications in addition to their capabilities to allow non–line–of sight (NLOS) propagation. Moreover, in inconvenient weather conditions such as rain, dust and fog, THz signals act as substitutes [6].

Deploying flying platforms in the communication network such as UAVs or drones is explosively increasing. Because of their inherent flexibility and mobility capabilities, UAVs are highly demanded in various potential applications in wireless systems in areas that exhibits no or insufficient terrestrial infrastructure. In other words, UAVs act as aerial base stations for the sake of increasing coverage, improving reliability, energy efficiency and boosting capacity of wireless networks [7], [8]. Compared to other airborne solutions such as helikite and high altitude platforms (HAP), deploying UAV–enabled wireless communication has a bunch of advantages. For instance, UAVs are always on–demand and easily deployed in any already existing network [9]. Also, UAV–enabled wireless communication offers superior link quality in the existence of shorter distance LOS communication channels with communicating ground nodes. Most importantly, UAVs offer high network flexibility with the fully controllable UAV's position in three dimensional (3D) airspace. For the potential advantages, UAVs are employed as mobile relays to attain wireless connectivity between a couple of nodes with no existing direct communication link between them and the UAV's position can be manipulated to boost the communication performance [10]. One critical issue about UAV–enabled wireless communications lies in its limited on–board dedicated energy level, which in turn needs to be efficiently utilized to enhance the communication performance and support the UAV with needed energy to fly, simultaneously. One of the smartest and simplest ways, yet most energy–efficient, is to equip the UAV with passive RIS. Recently, the emerging technology of RIS has been introduced and implemented in wireless communications to promote the communication performance in diverse scenarios such as cognitive radio systems, simultaneous wireless information and power transfer and UAV communications [11], [12]. Fabricated of passive and meta–material–based reconfigurable elements, an RIS can adaptively reconfigure both the amplitude and the phase of the incident electromagnetic signal to reflect it towards the desired directions to mitigate interference and boost the network performance. The most important advantage

This work is supported by the DAAD and in part by the Federal Ministry of Education and Research (BMBF, Germany) within the 6G Research and Innovation Cluster 6G-RIC under Grant 16KISK020K, in co-operation between the department of telecommunications systems at TU Berlin and German University in Cairo.

of passive RIS is that, unlike other transmission typologies such as amplify and forward (AM), passive RIS does not consume any power, which is beneficial for developing green and cost–efficient communications [13]. Despite recently applying RIS in mmWave systems, the deployment of RIS for THZ communications is still at its infancy [13], [14].
There are handful papers from the literature dealing with RIS over the THz channel. The authors in [15] considered an RIS-assisted and UAV–supported THz communications, where the minimum average rate of user equipments (UEs) is maximized by optimizing the UAV's position, RIS phase shifts and the power control. In [16], the authors considered minimizing the transmission delay between the UAV and the UEs in the THz band while meeting the communication requirements of each user. In their paper, the optimal location of the UAV, the users' transmit power as well as the bandwidth of each user are are optimized. In [17], the authors considered an RIS–assisted UAV wireless system, where a user equipment (UE) communicates with a UAV via an RIS. Accordingly, they presented a theoretical framework for the outage performance of an RIS–assisted UAV wireless systems taking into account the effects of different types of fading and misalignment and transceiver hardware imperfections. However, in their scenario, the system only considers the two communicating nodes with no interference experienced in their network.

From the above discussions, it is noted that researchers did not yet focus on analyzing the outage probability of the uplink of mobile device (MD) to BS through a UAV equipped with an RIS in the THz channel in the presence of two underlaying D2D pairs. In this paper, we tackle this problem, where the contributions of our work are summarized as follows:

- We study an uplink RIS–assisted network in the THz frequency band, where one cellular user communicates with the BS through a UAV equipped with an RIS and in the presence of underlaying two D2D pairs.
- The outage probability of the link from the MD to the BS through RIS is derived in a closed form. The optimum position of the UAV that minimizes the outage probability is determined using Golden Search method.
- We propose optimal phase shift design for the RIS in the scenario under consideration to maximize the SINR achieved at the BS.

II. System and Channel Model

A. System Model

Consider an uplink single cell RIS–aided cellular network as shown in Fig. 1. It consists of one BS, one UAV, one MD and two D2D pairs that coexist and share the same frequency resources with the MD . The direct link between the MD and the BS is unattainable due to high loss resulting from long distances travelled or the existence of obstacles. Therefore,

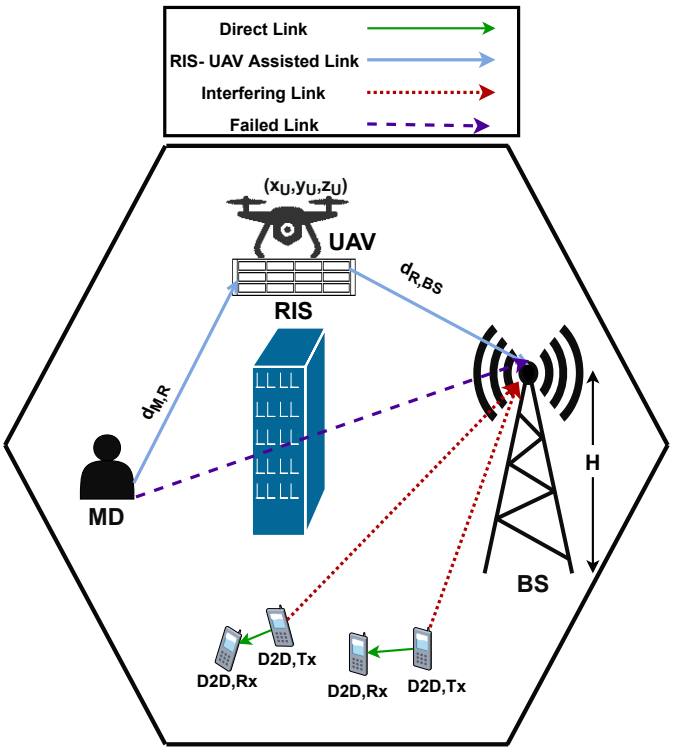

Fig. 1: Scenario under consideration where a UAV equipped with an RIS is deployed to assist the communication link between the MD and the BS in the existence of two underlaying D2D pairs.

a UAV equipped with an RIS is deployed in the network to establish communication links from the MD to the RIS and from the RIS to the BS and exploit the high mobility capabilities. RIS is a uniform planar array that consists of $N \times N$ extremely low cost reconfigurable passive reflecting elements. It reflects the incident waves from the MD and maps it to the BS, with directional beam with each element introducing a phase shift. With its reconfigurable capabilities, the propagation environment can be manipulated to enhance the system performance. Thanks to the RIS, the virtual link between the MD and BS is established through it. It is assumed that the BS is positioned in the X–Z plane with coordinates $\{x_{BS}, 0, H\}$, where H is the height of the BS. Furthermore, we assume that the MD and D2D pairs are positioned in the XY plane. So, the MD, i_{th} D2D transmitting and i_{th} receiving device have positions of $\{x_{MD}, y_{MD}, 0\}$, $\{x_{d2d_{tx_i}}, y_{d2d_{tx_i}}, 0\}$ and $\{x_{d2d_{Rx_i}}, y_{d2d_{Rx_i}}, 0\}$, respectively. Also, the n^{th} RIS array element has a position of $\{x_{R_n}, y_{R_n}, z_{R_n}\}$.
Consequently, the distance between the MD and RIS n_{th} element is given as:

$$d_{M,R_n} = \sqrt{(x_{MD} - x_{R_n})^2 + (y_{MD} - x_{R_n})^2 + z_{R_n}^2}, \quad (1)$$

Similarly, the distance between the BS and RIS n_{th} element is given as:

$$d_{R_n,BS} = \sqrt{(x_{R_n} - x_{BS})^2 + y_{R_n}^2 + (z_{R_n} - H)^2}. \quad (2)$$

The communication channels between the nodes in the network are assumed to be THz channels. All the channels between the nodes are assumed to be known or perfectly estimated. The description of this channel is provided in the next subsection.

B. Channel Model

In the following, the THz channel model is illustrated. It was developed utilizing THz wave atmospheric transmission attenuation model as well as water vapour absorption. The LOS THz channel gain is formulated as (9) in [18] :

$$h_{THz} = \sqrt{\frac{1}{PL(f,d)}}, \tag{3}$$

where $PL(f,d)$ is the pathloss that a signal with frequency f encounters when propagating a distance d.

$PL(f,d)$ counts for spreading loss $L_{sl}(f,d)$ and molecular absorption $L_{mal}(f,d)$ that feature the THz frequency band. The spreading loss $L_{sl}(f,d)$ is as a result of the expansion of the electromagnetic wave while propagating through different mediums. However, the molecular absorption $L_{mal}(f,d)$ is due to the collisions between atmospheric gas and/or water molecules. Comprehensive investigation on the effect of atmospheric attenuation was carried out in [19]. The channel coefficient h_{THz} follows zero-mean complex Gaussian distribution with variance that models free space path as well as molecular absorption gain. From [19] (Eqn. (2), (3) and (5)), the pathloss measured at frequency f when propagating a distance d is a function of the variance of the THz channel and is expressed as:

$$PL(f,d) = \frac{1}{\sigma^2} = \frac{1}{G_{Tx}G_{Rx}}(\frac{4\pi f d}{c})^2 e^{k(f)d}, \tag{4}$$

where σ^2 is the variance of the THz channel with zero mean. Hence, $h_{THz} \sim CN(0,\sigma^2)$. G_{Tx} is the transmitter antenna gain, G_{Rx} is the receiver antenna gain, c is the speed of light in free space and $k(f)$ represents the frequency dependent medium absorption factor that can be obtained from [20].

III. Mathematical Formulation

The received signal at the BS can be expressed as:

$$y_{BS} = \underbrace{\sqrt{P_M}\boldsymbol{h^T_{R,BS}\Theta h_{M,R}}X_M}_{\text{useful RIS–assisted signal}} + \sum_{i=1}^{2} \underbrace{\sqrt{P_{d2d_i}}h_{BS,d2d_i}X_{d2d_i}}_{\text{interference from transmitting D2Ds}} + \underbrace{n_o}_{\text{AWGN}}; \tag{5}$$

where $\boldsymbol{\Theta}$ is the phase shifts introduced by the RIS elements and is given by:

$$\boldsymbol{\Theta} = diag\{a_1 e^{j\theta_1}, ..., a_N e^{j\theta_N}\}; \tag{6}$$

where $\theta_n \in [0, 2\pi]$ and $a_n \in [0,1]$, P_M is the transmitting power of the MD, $\boldsymbol{h}_{R,BS}$ is the reflected channel gain sensed at BS from the RIS elements and has dimensions of $N \times 1$, $\boldsymbol{h}_{M,R}$ is the channel gain from the MD to the RIS elements and has dimensions of $N \times 1$, X_M is the transmitting signal of the MD and has unit energy, P_{d2d_i} is the transmitting power of D2D transmitting device i, $h_{BS,d2d_i}$ is the channel gain from D2D transmitting device i and the BS, X_{d2d_i} is the transmitting signal of transmitting device D2D i and has unit energy and n_o denotes the additive white Gaussian noise (AWGN) and has zero mean and variance N_o. For simplicity, we let the two D2D transmitting devices are assigned the same transmitting power P_{d2d}.

Using (5), the achieved SINR at the BS is expressed as:

$$SINR = \frac{P_M|\boldsymbol{h^T_{R,BS}\Theta h_{M,R}}|^2}{P_{d2d}\sum_{i=1}^{2}|h_{BS,d2d_i}|^2 + N_o}; \tag{7}$$

Let:

$$h^n_{M,R} = |h^n_{M,R}|e^{j\theta_M}; \tag{8a}$$

$$h^n_{R,BS} = |h^n_{R,BS}|e^{j\theta_{BS}}; \tag{8b}$$

To maximize the SINR at the BS expressed in (7), the optimal phase shift for RIS element n is chosen to maximize the SINR and is given as:

$$\theta^{opt}_n = -(\theta_M + \theta_{BS}); \tag{9}$$

Consequently, using (9), SINR given in (7) can be expressed as:

$$SINR = \frac{P_M|\sum_{n=1}^{N} a_n|h^n_{R,BS}||h^n_{M,R}||^2}{P_{d2d}\sum_{i=1}^{2}|h_{BS,d2d_i}|^2 + N_o}; \tag{10}$$

IV. Outage Probability Derivation

In this section, we derive the outage probability expression for the link between the MD and the BS. For simplicity, we let:

$$Y_n = a_n|h^n_{R,BS}||h^n_{M,R}|; \tag{11}$$

Since $|h^n_{M,R}|$ and $|h^n_{R,BS}|$ are independent random variables (i.r.v) and follow Rayleigh distribution with zero mean and variance $\sigma^2_{M,R}$ and $\sigma^2_{R,BS}$, the mean of Y_n, E[Y_n] and its variance Var[Y_n] are respectively given as:

$$E[Y_n] = a_n E[|h^n_{M,R}|]E[|h^n_{R,BS}|] = 0; \tag{12a}$$

$$Var[Y_n] = a_n^2 Var[|h^n_{M,R}|]Var[|h^n_{R,BS}|] = a_n^2\sigma^2_M\sigma^2_{BS}; \tag{12b}$$

where:

$$\sigma^2_{R,BS} = G_R G_{BS}(\frac{c}{4\pi f d_{R,BS}})^2 e^{-k(f)d_{R,BS}}, \tag{13a}$$

$$\sigma^2_{M,R} = G_M G_R(\frac{c}{4\pi f d_{M,R}})^2 e^{-k(f)d_{M,R}}, \tag{13b}$$

Let $X = \sum_{n=1}^{N} Y_n$. According to the central limit theorem (CLT), when the number of RIS elements is large enough, X converges to a Gaussian distribution. Accordingly, at a high value of N, X follows Gaussian distribution [21]. Therefore, the power density function (pdf) of X is given by:

$$Pr_{(MD\rightarrow BS)} = 1 - 24\lambda_1\lambda_2 e^{\frac{-2\gamma_{th}N_o}{3P_M\sigma_x^2}} \left\{ \frac{e^{\frac{\gamma_{th}N_o}{6P_M\sigma_x^2}}}{(12\lambda_1 + 6\frac{\gamma_{th}}{P_M\sigma_x^2})(12\lambda_2 + 6\frac{\gamma_{th}}{P_M\sigma_x^2})} + \frac{3}{(12\lambda_1 + 8\frac{\gamma_{th}}{P_M\sigma_x^2})(12\lambda_2 + 8\frac{\gamma_{th}}{P_M\sigma_x^2})} \right\}; \quad (14)$$

$$f_X(x) = \frac{1}{\sqrt{2\pi\sigma_X^2}} \exp\left(\frac{-x^2}{2\sigma_X^2}\right); \quad (15)$$

where

$$E(X) = \sum_{n=1}^{N} E[Y_n] = 0; \quad (16a)$$

$$Var(X) = \sigma_X^2 = \sum_{n=1}^{N} Var[Y_n]; \quad (16b)$$

Let the SINR expressed in (7) be written as:

$$SINR = \frac{Z}{V}; \quad (17)$$

where

$$Z = P_M|X|^2. \quad (18a)$$

$$V = P_{d2d}\sum_{i=1}^{2}|h_{BS,d2d_i}|^2 + N_o; \quad (18b)$$

In the following, the pdfs of Z and V are obtained. Z follows a Chi–squared distribution with zero mean and variance σ_X^2 which is given by:

$$f_Z(z) = \frac{1}{\sqrt{2\pi P_M\sigma_X^2 z}} \exp\left(\frac{-z}{2P_M\sigma_X^2}\right); \quad (19)$$

and since $|h_{BS,d2d_i}|^2$ follows an exponential distribution with zero mean and variance $\sigma_{BS,d2d_i}^2$, its pdf is given by:

$$f_{|h_{BS,d2d_i}|^2}(v) = \frac{1}{2\sigma_{BS,d2d_i}^2} \exp\left(\frac{-v}{2\sigma_{BS,d2d_i}^2}\right); \quad (20)$$

Since $|h_{BS,d2d_1}|^2$ and $|h_{BS,d2d_2}|^2$ are independent exponentially distributed random variables, V has a pdf given as [22]:

$$f_V(v) = \frac{\lambda_1\lambda_2}{\lambda_2 - \lambda_1}(e^{-\lambda_1(v-N_o)} - e^{-\lambda_2(v-N_o)}) \quad (21)$$

where

$$\lambda_1 = \frac{1}{2\sigma_{BS,d2d_1}^2}; \quad (22a)$$

$$\lambda_2 = \frac{1}{2\sigma_{BS,d2d_2}^2}; \quad (22b)$$

Based on the definition of outage probability, the outage probability of the link from the MD to the BS is expressed as:

$$Pr_{(MD\rightarrow BS)} = \iint\limits_{Z\leq\gamma_{th}V} f_{ZV}(z,v)dzdv \quad (23)$$

where $f_{ZV}(z,v)$ is joint pdf of Z and V and γ_{th} is the minimum SINR demanded at the BS to achieve a good quality of service (QoS) Since Z and V are independent, the outage probability of the link from the MD to the BS is expressed as:

$$Pr_{(MD\rightarrow BS)} = \int\limits_{N_o}^{\infty}\left[1 - 2Q(\frac{\sqrt{\frac{\gamma_{th}v}{P_M}}}{\sigma_x})\right]f_V(v)dv; \quad (24)$$

where $Q(y) = Pr(Y > y)$ is the probability that a standard normal random variable takes a value larger than y. Substituting (21) in (24) and performing some mathematical manipulations, $Pr_{(MD\rightarrow BS)}$ is expressed as:

$$Pr_{(MD\rightarrow BS)} = 1 - 2\frac{\lambda_1\lambda_2}{\lambda_2 - \lambda_1}\left[I_1 - I_2\right]; \quad (25)$$

where

$$I_1 = \int_{N_o}^{\infty} e^{-\lambda_1(v-N_o)}Q(\frac{\sqrt{\frac{\gamma_{th}v}{P_M}}}{\sigma_x})dv; \quad (26a)$$

$$I_2 = \int_{N_o}^{\infty} e^{-\lambda_2(v-N_o)}Q(\frac{\sqrt{\frac{\gamma_{th}v}{P_M}}}{\sigma_x})dv. \quad (26b)$$

To solve I_1 or similarly I_2, the approximation of $Q(\frac{\sqrt{\frac{\gamma_{th}v}{P_M}}}{\sigma_x})$ is used. One of the widely used approximation of $Q(x)$ is given by [23]:

$$Q(x) = \frac{1}{12}e^{\frac{-x^2}{2}} + \frac{1}{4}e^{\frac{-2x^2}{3}}\, x > 0; \quad (27)$$

By substituting (27) in (26a) and (26b) and after solving the integrations, I_1 and I_2 are expressed as:

$$I_1 = \frac{1}{12(\lambda_1 + \frac{\gamma_{th}}{2P_M\sigma_x^2})}e^{-\frac{\gamma_{th}N_o}{2P_M\sigma_x^2}} + \frac{1}{4(\lambda_1 + \frac{2\gamma_{th}}{3P_M\sigma_x^2})}e^{-\frac{2\gamma_{th}N_o}{3P_M\sigma_x^2}}; \quad (28a)$$

$$I_2 = \frac{1}{12(\lambda_2 + \frac{\gamma_{th}}{2P_M\sigma_x^2})}e^{-\frac{\gamma_{th}N_o}{2P_M\sigma_x^2}} + \frac{1}{4(\lambda_2 + \frac{2\gamma_{th}}{3P_M\sigma_x^2})}e^{-\frac{2\gamma_{th}N_o}{3P_M\sigma_x^2}}; \quad (28b)$$

By substitution of (28a) and (28b) in (25), the total outage probability is given by (14) at the top of this page, where λ_1 and λ_2 are given respectively in (22a) and (22b).

$$Pr_{(MD\rightarrow BS)} = 1 - 24\lambda_1\lambda_2 \exp\left(\frac{-2N_o\gamma_{th}}{3P_M N a_n A d_{M,U}^{-2} d_{U,BS}^{-2} e^{-k(f)(d_{M,U}+d_{U,BS})}}\right)\times$$
$$\left\{\frac{\exp\left(\frac{N_o\gamma_{th}}{6P_M N a_n A d_{M,U}^{-2} d_{U,BS}^{-2} e^{-k(f)(d_{M,U}+d_{U,BS})}}\right)}{\left(12\lambda_1 + \frac{6\gamma_{th}}{P_M N a_n A d_{M,U}^{-2} d_{U,BS}^{-2} e^{-k(f)(d_{M,U}+d_{U,BS})}}\right)\left(12\lambda_2 + \frac{6\gamma_{th}}{P_M N a_n A d_{M,U}^{-2} d_{U,BS}^{-2} e^{-k(f)(d_{M,U}+d_{U,BS})}}\right)} + \right. \tag{29}$$
$$\left.\frac{3}{\left(12\lambda_1 + \frac{8\gamma_{th}}{P_M N a_n A d_{M,U}^{-2} d_{U,BS}^{-2} e^{-k(f)(d_{M,U}+d_{U,BS})}}\right)\left(12\lambda_2 + \frac{8\gamma_{th}}{P_M N a_n A d_{M,U}^{-2} d_{U,BS}^{-2} e^{-k(f)(d_{M,U}+d_{U,BS})}}\right)}\right\}.$$

V. UAV Positioning Optimization

In this subsection, we obtain the UAV's position that minimizes the total outage probability given in (14). It is considered that the UAV's flight is at a fixed altitude h and the UAV moves horizontally to update its position according to the given scenario. Therefore, the UAV's position (x_U, y_U, h) needs to be optimized to minimize the outage probability expressed in (14). Substituting (12b) and (16b) in (14) and assuming that the distances travelled by the UAV are very large compared to the distance between RIS elements, the achieved outage probability at the BS is expressed in (29) at the top of this page, where A is given as:

$$A = G_M G_{BS} \frac{C^4}{(4\pi)^4}; \tag{30}$$

The distances between the MD and the UAV and that from the UAV to the BS are given respectively as:

$$d_{M,U}(x_U, y_U) = \sqrt{(x_{MD} - x_U)^2 + (y_{MD} - x_U)^2 + z_U^2},$$
$$d_{U,BS}(x_U, y_U) = \sqrt{(x_U - x_{BS})^2 + y_U^2 + (z_U - H)^2}.$$

We use two–dimensional (2D) Golden Search method within an acceptable tolerance ϵ to minimize the outage probability expressed in (29) in terms of the UAV x–and y–coordinates, x_U and y_U, respectively (given that h is fixed) or equivalently maximize $F(x_U, y_U)$, where $F(x_U, y_U) = -Pr_{(MD\rightarrow BS)}$.

This maximization is performed iteratively using Golden Search method and is summarized in Algorithm 1. The algorithm begins with initializing the input value of the tolerance ϵ and bounds of $F(x_U, y_U)$. In each iteration, the search interval $\Delta x = x^u - x^l$ and $\Delta y = y^u - y^l$ reduced by a factor of 0.618 given that x^l and y^l are the lower bounds, but x^u and y^u are the upper bounds of the UAV's position coordinates x_U and y_U. Initially, the values of the lower bounds are set to $x^l = y^l = 0$, where the upper bounds are set to $x^u = x_{max}$ and $y^u = y_{max}$, where it is assumed that the area under investigation is a rectangle of sides equal to x_{max} and y_{max}. In the first iteration, the four points are evaluated and corresponding values of $F(x_U, y_U)$, namely F_1, F_2, F_3 and F_4 are then computed. Depending on the maximum values, the intervals alter in order to search for the optimum point that would maximize $F(x_U, y_U)$. After that, again their values are then evaluated for the following iteration till a number of iterations N_{loop}, at which one of the intervals Δx and Δy is greater than the acceptable tolerance ϵ. In fact, this can be expressed as $\max(\Delta x, \Delta y)(0.618)^{N_{loop}} \geq \epsilon$. Eventually, the algorithm ends up obtaining the optimal UAV x–and y–coordinates x_U^* and y_U^* respectively that maximize F_{x_U, y_U} or equivalently minimizes the outage probability at the BS expressed in (29).

VI. Performance Evaluation and Numerical Results

In this section, numerical results are provided to validate the analytical results of outage probability and position optimization for uplink RIS and UAV–assisted communication system in THz frequency band and in the presence of underlaying D2Ds. The effect of some system parameters on the derived outage probability is studied. We assume a square area for the deployment of all links with an edge of 50 m. Also, it is assume also that the two pairs of D2D devices are uniformly and randomly distributed in the X–Y plane in the specified square area. The MD is located in the X–Y plane, while the BS is located in the X–Z plane. The UAV that is equipped with RIS is initially located somewhere between the MD and the BS with a fixed height. The values of the simulation parameters are summarized in Table I.

In Fig.2, the outage probability of four different schemes (shown in the figure) are plotted versus γ_{th} that guarantees achieving good QoS at the range from zero to 1. The MD power P_M is set to 0.05 W and the number of RIS elements N is set to 36. From the figure, it is shown that as γ_{th} increases, the outage probability measured at the BS increases. This is due to increasing the system requirements within the available power budget assigned to P_M that leads to increasing the probability of link failure from MD to the BS. Additionally, the best performance is obtained when both the phase shifts of the RIS as well as the UAV's position are optimized, namely "Opt. Phase Shifts and Opt. UAV Position".

Algorithm 1: Iterative minimization of $Pr_{(MD \rightarrow BS)}$ using Golden Search method

Input: Tolerance ϵ, UAV position bounds x^l, x^u, y^l and y^u
Output: Optimal UAV Position x_U^* and y_U^*

Calculate $x^p \leftarrow x^u - 0.618(x^u - x^l)$,
$x^q \leftarrow x^l + 0.618(x^u - x^l)$,
$y^p \leftarrow y^u - 0.618(y^u - y^l)$,
$y^q \leftarrow y^l + 0.618(y^u - y^l)$.
Calculate $F_1 \leftarrow F(x^p, y^p)$, $F_2 \leftarrow F(x^q, y^p)$,
$F_3 \leftarrow F(x^p, y^q)$, $F_4 \leftarrow F(x^q, y^q)$
Calculate $\Delta x \leftarrow x^u - x^l$, $\Delta y \leftarrow y^u - y^l$
while $max(\Delta x, \Delta y) > \epsilon$ **do**
  if $F_1 == max(F_1, F_2, F_3, F_4)$ **then**
    Set $x^u \leftarrow x^q$, $x^q \leftarrow x^p$,
    $y^u \leftarrow y^q$,$y^q \leftarrow y^p$
    Calculate $x^p \leftarrow x^u - 0.618(x^u - x^l)$,
    $y^p \leftarrow y^u - 0.618(y^u - y^l)$
  else
    if $F_2 == max(F_1, F_2, F_3, F_4)$ **then**
      Set $x^l \leftarrow x^p$, $x^p \leftarrow x^q$, $y^u \leftarrow y^q$, $y^q \leftarrow y^p$
      Calculate $x^q \leftarrow x^l + 0.618(x^u - x^l)$,
      $y^p \leftarrow y^u - 0.618(y^u - y^l)$
    else
      if $F_3 == max(F_1, F_2, F_3, F_4)$ **then**
        Set $x^u \leftarrow x^q$, $x^q \leftarrow x^p$, $y^l \leftarrow y^p$, $y^p \leftarrow y^q$
        Calculate $x^p \leftarrow x^u - 0.618(x^u - x^l)$,
        $y^q \leftarrow y^l + 0.618(y^u - y^l)$
      else
        Set $x^l \leftarrow x^p$, $x^p \leftarrow x^q$, $y^l \leftarrow y^p$, $y^p \leftarrow y^q$
        Calculate $x^q \leftarrow x^l + 0.618(x^u - x^l)$
        $y^q \leftarrow y^l + 0.618(y^u - y^l)$
  Calculate $F_1 \leftarrow F(x^p, y^p)$,
  $F_2 \leftarrow F(x^q, y^p)$,
  $F_3 \leftarrow F(x^p, y^q)$,
  $F_4 \leftarrow F(x^q, y^q)$
Calculate $x_U^* = \frac{x^l + x^u}{2}$,
$y_U^* = \frac{y^l + y^u}{2}$,
$F^* = F(x_U^x, y_U^*)$.

TABLE I: Simulation Parameters.

Parameter	Description	Value
f	Operating Frequency	1 THz
$k(f)$	Absorption Coefficient	0.1
N_o	Noise Variance	-40 dB
H	BS height	10 m
h	UAV altitude	20 m
a_n	RIS element Amplitude	1
ϵ	Convergence Tolerance	10^{-3}

This best performance is then followed by the "Random Phase Shifts and Opt. UAV Position" scheme, where the

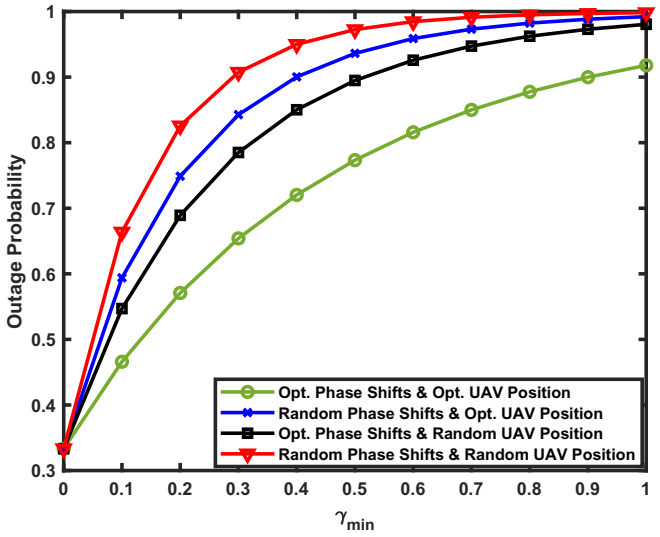

Fig. 2: Outage Probability versus γ_{th} for 4 Different Schemes.

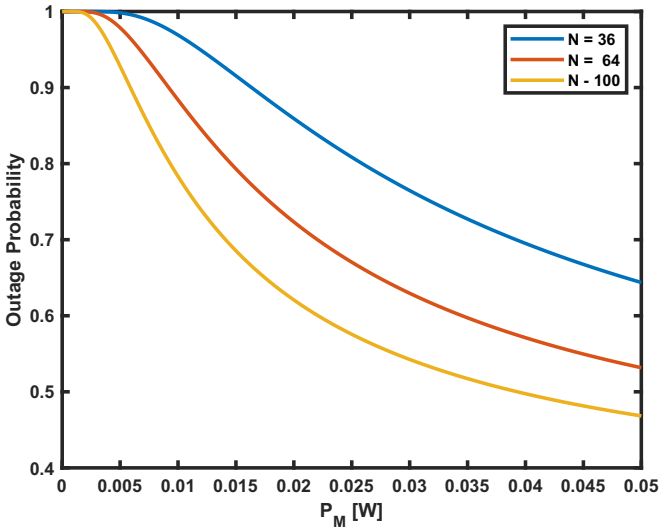

Fig. 3: Outage Probability versus P_M at Different Values of RIS elements.

UAV's Position is optimized according to the given scenario to lessen the outage probability achieved at the BS while the RIS elements are assigned random phase shifts. Then comes the "Opti Phase Shifts and Not Opt. UAV Position" scheme, where only the RIS elements' phase shifts are optimized to maximize the SINR at the BS, while the UAV is randomly positioned between the MD and the BS. The highest outage probability is achieved by the "Random Phase Shifts and Not Opt. UAV Position", where both the UAV's position and the RIS elements' phase shifts are randomly assigned. This highlights the effectiveness of the RIS phase shifts and UAV's position optimization scheme and proves the high role the UAV's mobility plays in UAV–enabled networks.

In Fig. 3, the outage probability of the communication

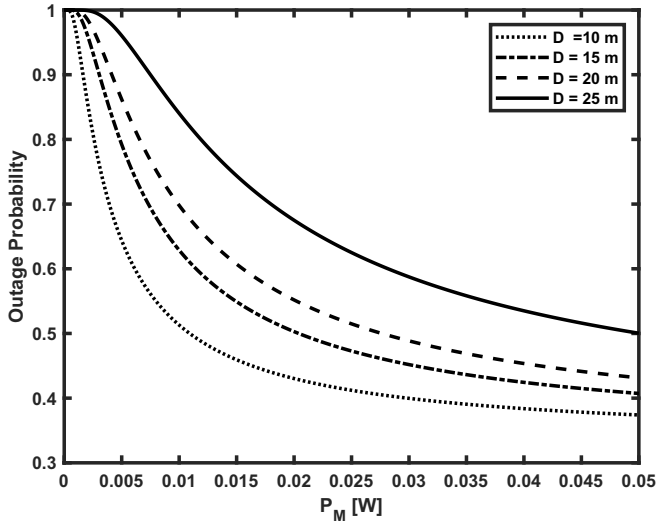

Fig. 4: Outage Probability versus P_M at Different Distances between MD and BS.

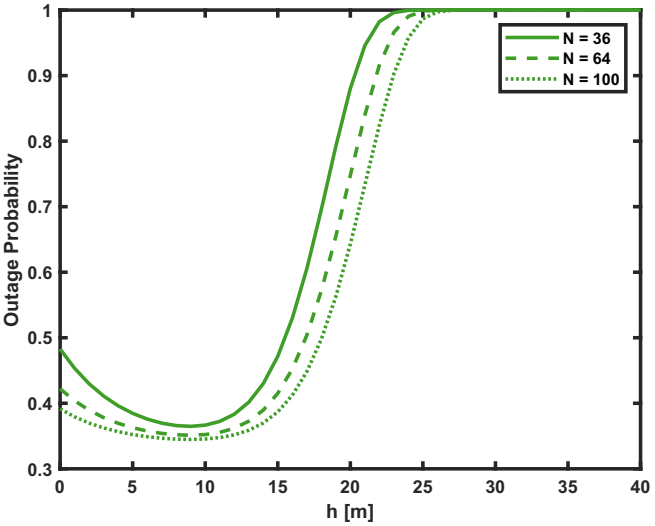

Fig. 5: Outage Probability versus UAV Altitude h at Different Number of RIS elements N.

link from MD to BS through RIS is plotted versus the MD transmitting power P_M for different number of RIS elements $N = 36$, 64 and 100 at γ_{th} of 0.5. As expected, the figure depicts a decrease in the achieved outage probability when increasing the MD dedicated power P_M. This is because the increase of P_M allows higher transmit power for the MD and the UAV which causes a decrease in the outage probability. Moreover, it is noted that as N increases, the outage probability decreases. This in turn proves the effectiveness of deploying passive RIS–assisted network so that phase shifts introduced by the channel can be eliminated.

In Fig. 4, the outage probability of the communication link from MD to BS through RIS is plotted versus the MD transmitting power P_M at different distances D = 10, 15, 20 and 25 m between the MD and the BS for $N = 36$. As the figure depicts, increasing the distance between the MD and the BS results in an increase in the outage probability. This is due to the higher pathloss that the propagating signal experiences at a longer travelling distance which is considered one of the challenges of THz communications. This problem can be solved by equipping the BS with MIMO system that contributes in improving the QoS significantly.

Fig. 5 shows the outage probability for the proposed scheme versus the UAV altitude h. As before, the higher the number of RIS elements N, the lower the outage probability is achieved. Also, it is noticed that the outage probability for the proposed scheme decreases whenever the UAV altitude h increases until $h \approx 10\ m$ which is equal to the height of the BS. This value corresponds to a shorter distance between the UAV and the BS, $D_{R,BS}$. Whenever h increases forward, $D_{R,BS}$ increases. This in turn causes excess power loss and accordingly leads to an increase in the outage probability due to an increase in the distance between the UAV and the BS.

VII. Conclusions

In this paper, the outage probability of an uplink RIS–assisted one cell communication system is considered in the existence of two underlaying D2D devices, where the RIS is attached to a UAV that adapts its position for better channel conditions and hence higher system performance and better QoS. The system is evaluated in terms of the outage probability. A closed form expression for the outage probability is derived. The optimal phase shifts for the RIS elements are obtained to improve the system performance. Furthermore, the UAV's position is optimized to minimize the derived outage probability. Numerical results show the effectiveness of optimizing the RIS elements' phase shits and the UAV's position as compared to assigning them randomly. Additionally, increasing the number of RIS elements leads to improving the system performance, which in turn proves the effectiveness of deploying passive RIS–assisted network.

References

[1] C. Han, L. Yan, and J. Yuan, "Hybrid beamforming for terahertz wireless communications: Challenges, architectures, and open problems," *IEEE Wireless Communications*, vol. 28, no. 4, pp. 198–204, 2021.

[2] R. Singh and D. Sicker, "Thz communications-a boon and/or bane for security, privacy, and national security," in *TPRC48: The 48th Research Conference on Communication, Information and Internet Policy*, 2020.

[3] H.-J. Song and T. Nagatsuma, *Handbook of terahertz technologies: devices and applications*. CRC press, 2015.

[4] M. Sung, S.-R. Moon, E.-S. Kim, S. Cho, J. K. Lee, S.-H. Cho, T. Kawanishi, and H.-J. Song, "Design considerations of photonic thz communications for 6g networks," *IEEE Wireless Communications*, vol. 28, no. 5, pp. 185–191, 2021.

[5] A.-A. A. Boulogeorgos, A. Alexiou, D. Kritharidis, A. Katsiotis, G. Ntouni, J. Kokkoniemi, J. Lethtomaki, M. Juntti, D. Yankova, A. Mokhtar, J.-C. Point, J. Machado, R. Elschner, C. Schubert, T. Merkle, R. Ferreira, F. Rodrigues, and J. Lima, "Wireless terahertz system architectures for networks beyond 5g," *CoRR*, vol. abs/1810.12260, 2018. [Online]. Available: http://arxiv.org/abs/1810.12260

[6] H. Elayan, O. Amin, R. M. Shubair, and M.-S. Alouini, "Terahertz communication: The opportunities of wireless technology beyond 5g," in *2018 International Conference on Advanced Communication Technologies and Networking (CommNet)*. IEEE, 2018, pp. 1–5.

[7] S. K. Khan, M. Farasat, U. Naseem, and F. Ali, "Performance evaluation of next-generation wireless (5g) uav relay," *Wireless Personal Communications*, vol. 113, no. 2, pp. 945–960, 2020.

[8] S. Hosseinalipour, A. Rahmati, and H. Dai, "Interference avoidance position planning in uav-assisted wireless communication," in *ICC 2019-2019 IEEE International Conference on Communications (ICC)*. IEEE, 2019, pp. 1–6.

[9] Y. Zeng and R. Zhang, "Energy-efficient uav communication with trajectory optimization," *IEEE Transactions on Wireless Communications*, vol. 16, no. 6, pp. 3747–3760, 2017.

[10] Y. Zeng, J. Xu, and R. Zhang, "Energy minimization for wireless communication with rotary-wing uav," *IEEE Transactions on Wireless Communications*, vol. 18, no. 4, pp. 2329–2345, 2019.

[11] M. Di Renzo, K. Ntontin, J. Song, F. H. Danufane, X. Qian, F. Lazarakis, J. De Rosny, D.-T. Phan-Huy, O. Simeone, R. Zhang *et al.*, "Reconfigurable intelligent surfaces vs. relaying: Differences, similarities, and performance comparison," *IEEE Open Journal of the Communications Society*, vol. 1, pp. 798–807, 2020.

[12] S. Abeywickrama, R. Zhang, Q. Wu, and C. Yuen, "Intelligent reflecting surface: Practical phase shift model and beamforming optimization," *IEEE Transactions on Communications*, vol. 68, no. 9, pp. 5849–5863, 2020.

[13] Z. Wan, Z. Gao, F. Gao, M. Di Renzo, and M.-S. Alouini, "Terahertz massive mimo with holographic reconfigurable intelligent surfaces," *IEEE Transactions on Communications*, vol. 69, no. 7, pp. 4732–4750, 2021.

[14] S. Liu, Z. Gao, J. Zhang, M. Di Renzo, and M.-S. Alouini, "Deep denoising neural network assisted compressive channel estimation for mmwave intelligent reflecting surfaces," *IEEE Transactions on Vehicular Technology*, vol. 69, no. 8, pp. 9223–9228, 2020.

[15] Y. Pan, K. Wang, C. Pan, H. Zhu, and J. Wang, "Uav-assisted and intelligent reflecting surfaces-supported terahertz communications," *IEEE Wireless Communications Letters*, vol. 10, no. 6, pp. 1256–1260, 2021.

[16] L. Xu, M. Chen, M. Chen, Z. Yang, C. Chaccour, W. Saad, and C. S. Hong, "Joint location, bandwidth and power optimization for thz-enabled uav communications," *IEEE Communications Letters*, vol. 25, no. 6, pp. 1984–1988, 2021.

[17] A.-A. A. Boulogeorgos, A. Alexiou, and M. Di Renzo, "Outage performance analysis of ris-assisted uav wireless systems under disorientation and misalignment," *arXiv preprint arXiv:2201.12056*, 2022.

[18] H. Zhang, H. Zhang, W. Liu, K. Long, J. Dong, and V. C. Leung, "Energy efficient user clustering, hybrid precoding and power optimization in terahertz mimo-noma systems," *IEEE Journal on Selected Areas in Communications*, vol. 38, no. 9, pp. 2074–2085, 2020.

[19] A.-A. A. Boulogeorgos, E. N. Papasotiriou, and A. Alexiou, "A distance and bandwidth dependent adaptive modulation scheme for thz communications," in *2018 IEEE 19th International Workshop on Signal Processing Advances in Wireless Communications (SPAWC)*. IEEE, 2018, pp. 1–5.

[20] J. M. Jornet and I. F. Akyildiz, "Channel Modeling and Capacity Analysis for Electromagnetic Wireless Nanonetworks in the Terahertz Band," *IEEE Transactions on Wireless Communications (TWC)*, vol. 10, no. 10, pp. 3211–3221, Oct. 2011.

[21] D. Kudathanthirige, D. Gunasinghe, and G. Amarasuriya, "Performance analysis of intelligent reflective surfaces for wireless communication," in *ICC 2020-2020 IEEE International Conference on Communications (ICC)*. IEEE, 2020, pp. 1–6.

[22] P. Oguntunde, O. Odetunmibi, and A. Adejumo, "On the sum of exponentially distributed random variables: A convolution approach," *European Journal of Statistics and Probability*, vol. 2, no. 1, pp. 1–8, 2014.

[23] D. N. Phong, N. X. Hoai, R. I. McKay, C. Siriteanu, N. Q. Uy, and N. Park, "Evolving the best known approximation to the q function," in *Proceedings of the 14th annual conference on Genetic and evolutionary computation*, 2012, pp. 807–814.